A. GORIACHKO, P.V. MELNIK, M.G. NAKHODKIN

Department of Physical Electronics, Taras Shevchenko National University of Kyiv
(4G, Academician Glushkov Ave., Kyiv 03022, Ukraine; e-mail: andreandy2000@gmail.com)

NEW FEATURES OF THE Ge(111) SURFACE WITH CO-EXISTING c(2 × 8) AND 2 × 2 RECONSTRUCTIONS INVESTIGATED BY SCANNING TUNNELING MICROSCOPY

UDC 539

The c(2 × 8) ground state reconstruction of the Ge(111) surface can be easily disrupted by the 2×2 reconstruction, since both of them are rather close to each other in terms of the surface free energy. Both structures are comprehensively studied in the literature. However, new surface features can be found on the borders between c(2×8) and 2×2 domains of various registries and orientations. We report scanning tunneling microscopy observations and suggest atomic models for the linear chains of 2×2 cells or c(2×4) cells, as well as adatom/restatom group vacancies, including corner holes of a similar geometry, like the case of the Si(111)-7 × 7 surface.

K e y w o r d s: germanium, surface, reconstruction, scanning tunneling microscopy.

1. Introduction

The semiconductor surface reconstruction is an outstanding phenomenon of the thermodynamically driven nanostructuring in the process of reaching a minimum of the surface free energy [1]. Three principles govern the reconstruction of clean low-index faces of tetrahedrally coordinated elemental semiconductors: 1. Surface dangling bonds are saturated by rehybridization or conversion to non-bonding states; 2. The surface tries to lower its energy by atomic relaxations leading to the spectrum of surface electronic states with a band gap; 3. The surface structure will be of the lowest free energy kinetically accessible under the given preparation conditions. The most famous example is the 7 × 7 dimer – adatom – stacking fault (DAS) reconstruction of the Si(111) surface [2, 3], which is now a de-facto standard of the surface science in textbooks, a test sample for various experimental techniques, and a well-defined substrate for epitaxy, nanoscale film growth, or molecular arrays.

A closely related Ge(111) surface has attracted a far less attention, as its c(2×8) reconstruction [4, 5] is considered to be simply a trivial adatom decoration of the bulk lacking surface dimers, stacking faults, and corner holes. The formation of the c(2×8) superstructure takes place, when atomically clean Ge(111) is annealed in an ultra-high vacuum (UHV) environment at a temperature high enough for the essential melting of the topmost atomic layer, followed by cooling down to room temperature, which is slow enough for the surface to be frozen in the lowest energy state. This is in contrast to the surface preparation by cleaving in UHV, when the surface atoms are deprived of mobility and the Ge(111)-2 × 1 reconstruction is formed [6]. References to earlier works on the Ge(111) surface structures, as well as transitions between different phases, as the temperature varies, can be found in the review by Duke [1].

Unlike the Si(111)-7 × 7, the Ge(111)-c(2 × 8) reconstruction can be easily disrupted by the 2 × 2 superstructure, which is itself also a stable atomic arrangement, although not a global minimum of system's energy [7]. Small patches of the 2 × 2 structure

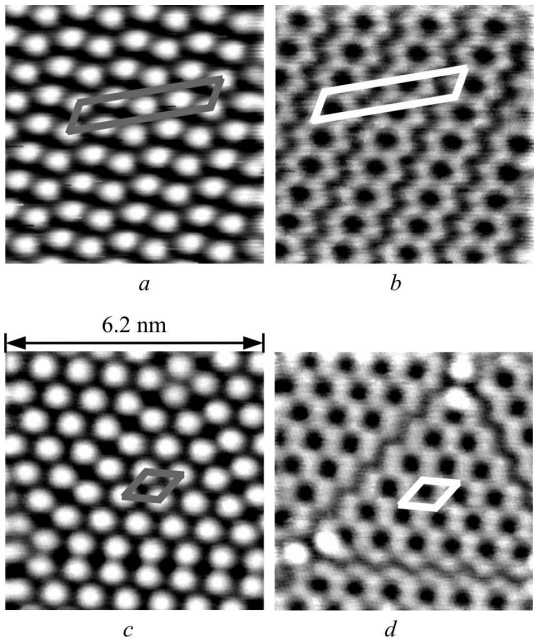

Fig. 1. STM images (6.2 nm × 6.2 nm field of view) of the atomically flat Ge(111) reconstructed surface after the standard preparation procedure. The same area amidst the c(2×8) domain imaged in the empty states (*a*) (the sample bias voltage: +1.5 V) and the occupied state (–1.5 V) (*b*). Grey and white parallelograms outline the c(2 × 8) unit cell. The same area amidst the 2×2 domain imaged in the empty states (+2 V) (*c*) and the occupied states (–2 V) (*d*). Grey and white rhombs outline the 2 × 2 unit cell

were observed, indeed, by means of scanning tunneling microscopy (STM) on the Ge(111) substrate in the co-existence with the predominant c(2 × 8) surface coverage [4, 5, 8, 9]. From purely geometric considerations, it is evident that the c(2 × 8)/(2 × 2) combination can lead to the existence of numerous nanoscale features, which were not investigated systematically so far. Rather, the previous investigations were focused on various point defects on the Ge(111)-c(2 × 8) by means of scanning tunneling microscopy (STM) [8, 9]. The STM is the most appropriate technique for the observation of atomic and nano-sized defects on semiconductor surfaces. Thus, it was chosen in the present work for the characterization of the boundaries between various c(2×8) and 2×2 domains.

2. Experimental

Our investigation was performed in a UHV chamber with a base pressure of 2×10^{-10} mbar equipped with a home-built STM [10] and Auger electron spectrometer. We have used standard microelectronics-grade polished Ge(111) wafers (*p*-type, Ga-doped, 0.3 Ω · cm). The atomically clean Ge(111) reconstructed surface was prepared by the repeated bombardment by 500-eV Ar^+ at 300 K and by the annealing at 900 K. A slow cooling (for 10 min) to 300 K was practiced after the final annealing step. The presence of any contaminations on the surface was monitored by Auger electron spectroscopy (AES), while the ion bombardment and the annealing of a sample were continued until all contaminants were reduced below the detection limit of AES. The STM images were obtained at 300 K in the constant current mode (typical tunneling current 0.3 nA). Probe tips were made of a platinum-iridium wire (80% Pt, 20% Ir) by means of a simple mechanical cutting, followed by the electron bombardment in UHV with 2.5 kV voltage applied between the tip and the cathode.

3. Ge(111)-c(2 × 8) vs Ge(111)-(2 × 2)

The sample preparation described above has yielded a high quality Ge(111) reconstructed surface with terraces up to 100 nm in width and predominant coverage by the c(2 × 8) domains with low defect density. A representative example of the STM images obtained on such domain is presented in Fig. 1, *a* (empty states) and Fig. 1, *b* (occupied states). Figure 1, *a*–*b* shows the same surface area imaged at opposite tunneling bias voltage polarities, the c(2 × 8) unit cell is outlined by grey and white parallelograms. Their short and long sides have 0.8 nm and 3.2 nm length, correspondingly, which are equal to 2 and 8 in-plane unit lengths (0.4 nm) of the bulk-like terminated Ge(111). The difference between the images of empty and occupied states stems from the specific spatial distribution of the electronic density of states (will be discussed shortly). Figure 1, *a*–*b* is fully consistent with STM images of the Ge(111)-c(2 × 8) reported in the literature by other authors [4, 5, 8, 9, 11, 12], as well as with the earlier results of low energy electron diffraction (LEED) [13].

A minority of locations on the surface of our samples displayed patches of the 2 × 2 superstructure, as exemplified by Fig. 1, *c*–*d*. Here, the same area inside the 2 × 2 domain is imaged both in empty (*c*, +2 V) and occupied (*d*, –2 V) states, the 2 × 2 unit cell is outlined by grey and white rhombs on

both STM images. Their sides of 0.8 nm are twice as long as the 0.4-nm in-plane periodicity of the bulk-like non-reconstructed Ge(111). The different appearances of the 2×2 superstructure in empty and occupied states is similar to the basic Ge(111)-c(2×8) case. Our STM images are in qualitative agreement with the theoretically predicted STM images of the Ge(111)-2×2 [14]. We also observe the absence of a long-range order in Fig. 1, *c–d* manifesting itself in a small size of the 2×2 domains, typically in the sub 10 nm range.

No sample was observed in our experiments completely without the 2×2 domains. Thus, we consider the later as an intrinsic feature of the Ge(111) surface. We speculate that unavoidable irregularities of the surface crystalline structure, which are caused by steps, bulk defects, etc. can be responsible for tipping the energy balance in favor of the 2×2 superstructure in certain locations. Due to a small partial area and the incoherent placement of 2×2 domains on the regular Ge(111) sample, it is hard to expect the detection of this phase by means of the LEED technique. However, the LEED observation of the 2×2 domains was reported on the strongly miscut Ge(111), where an immediate vicinity of steps stabilized the 2×2 instead of the c(2×8) on extremely small terraces over sample's surface [15].

The widely accepted atomic models of the Ge(111)-c(2×8) and Ge(111)-2×2 are sketched in Fig. 2, *a* and *b*, correspondingly [4, 5, 7–9, 11, 12, 16]. They differ in the pattern of decoration of the bulk-like (non-reconstructed) Ge(111) surface by Ge "adatoms", provided the quantity of the latter being not enough to complete the next atomic layer. The rationale for the positioning of adatoms is reducing the number of dangling bonds on the reconstructed surface, which, in its turn, minimizes the free energy of the system. Each adatom saturates three dangling bonds of the surface atoms by forming chemical bonds with them. This yields one dangling bond (on the adatom itself) instead of three, and the corresponding three surface atoms are, thus, called "backbond atoms". Not all surface atoms can saturate their dangling bonds by the arrangement of neither adatoms of c(2×8) nor that of 2×2. The atoms of the first surface atomic layer with the remaining dangling bonds are designated as "restatoms".

The restatoms differ from adatoms by the local density of electronic states, resulting in the substantially different appearance of the surface on the STM images of empty and occupied states (see Fig. 1, *a, c* vs. *b, d*). Namely, only adatoms are visible in the images of empty states, while both adatoms and restatoms contribute to the formation of the image of occupied states. This is a result of the electron transfer from adatoms' dangling bonds to restatoms' dangling bonds, leading to the formation of filled and empty surface state bands with the predominant localization on restatoms and adatoms, correspondingly. In terms of the hybridization of orbitals, the dangling bonds on restatoms and adatoms become more like *s*- and *p*-type, correspondingly, whereas, in

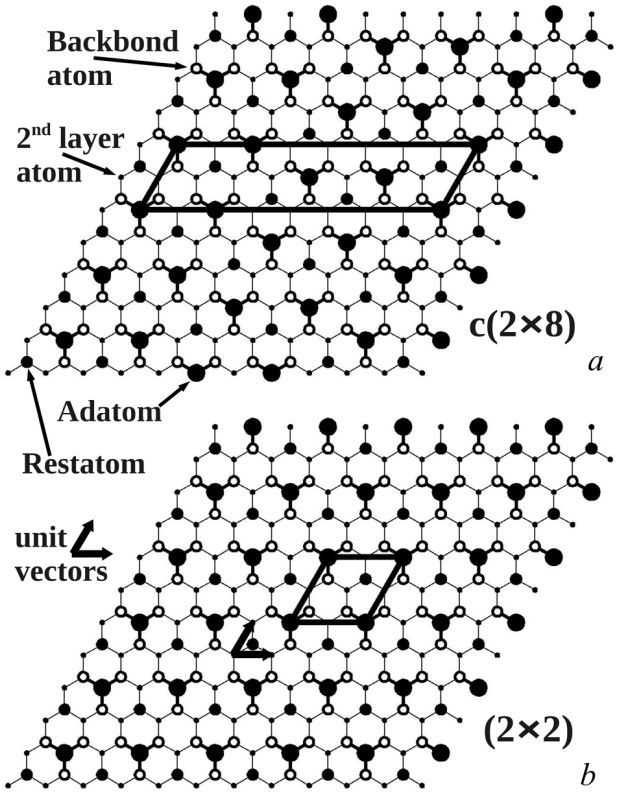

Fig. 2. Top views of ball-and-stick atomic models of the Ge(111) reconstructions: c(2×8) (*a*), and 2×2 (*b*). The size of an atom represents (but not proportional to) how close it is to the reader. Small black dots correspond to the 2nd layer atoms. The first (basic surface) layer consists of the so-called "backbond atoms" (small empty circles) and "restatoms" (small black filled circles). The surface is decorated by the so-called "adatoms", which are depicted by large black filled circles. The c(2×8) and 2×2 unit cells are outlined by a black line. Small black arrows are in-plane unit vectors of the bulk-like (non-reconstructed) Ge(111) crystallographic plane

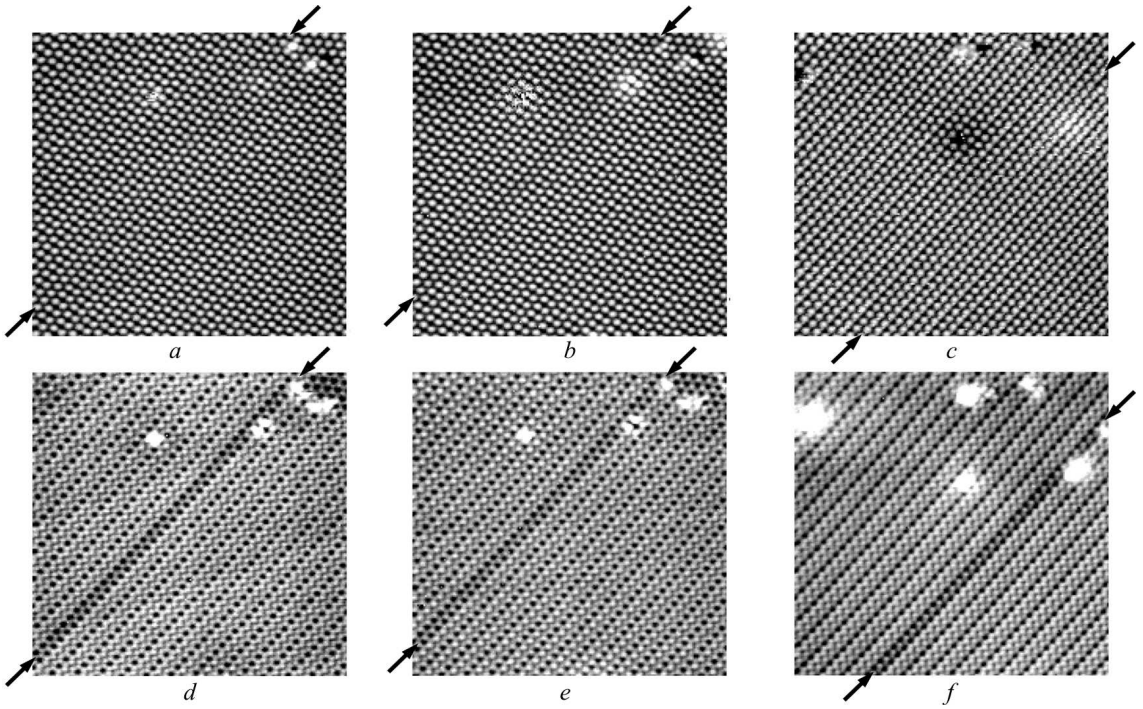

Fig. 3. STM images of the Ge(111)-c(2 × 8) terrace with several localized defects and a linear defect in the form of a row of 2 × 2 cells in empty and occupied states. All images are 25 nm × 25 nm in size and show the same area on the sample except for some shifts due to the thermal drift. Sample bias voltages are: +2.5 V (*a*); +1.5 V (*b*); +0.8 V (*c*); −2.5 V (*d*); −1.5 V (*e*); −0.8 V (*f*). Tunneling current: 0.3 nA. In every panel, the two points on the perimeter of the image, which define the line of 2 × 2 cells, are designated by black arrows

the bulk of a germanium crystal, each atom has four identical sp^3-type orbitals [1].

4. 1D Chains of 2 × 2 Cells

Small 2×2 domains, whose typical example is given in Fig. 1, *c*–*d*, are not the only possibility to disrupt the ideal Ge(111)-c(2×8) superstructure. An early X-ray diffraction study by Feidenhans'l *et al.* [17] led to the conclusion about the fault in the form of rows of 2×2 unit cells. Our carefull observation in the real space has revealed such linear chains of 2 × 2 cells amidst an atomically flat terrace with low number of defects. The STM images of such a terrace obtained at different bias voltages are presented in Fig. 3. Here, the two points, which define the line of the fault, are marked by black arrows on the periphery of the image in every panel.

In the images of empty states (Fig. 3, *a*–*c*), only adatoms are imaged, and the fault manifests itself as a row of extra adatoms running in the [1$\bar{1}$0] direction or, alternatively, as a straight line of 2 × 2 supercells sandwiched between two extended c(2 × 8) domains. Both adatoms and restatoms contribute to the image formation in occupied states, however, to different degrees depending on the bias magnitude, which is further complicated by inequivalences inside the populations of adatoms and restatoms (there are non-equivalent adatoms and non-equivalent restatoms within the c(2 × 8) unit cell due to non-equivalent geometries of their atomic surroundings) (Fig. 3, *d*–*f*). The general feature of these images of occupied states is a clear visibility of the structural fault in the form of a linear stripe of lowered brightness against the regular c(2 × 8) background. This means that such 2 × 2 row is characterized by the density of occupied electronic states lower than that for the surrounding, which can be dubbed as "quantum antiwire".

The atomic model of a linear 2 × 2 chain is presented in Fig. 4, *a*, where all 2×2 cells are delineated with a dashed line. It is important to realize that the

c(2 × 8) domains to the left and to the right from the chain are not in registry with each other, d being the off-registry shift parallel to the longer side of the unit cell. In our model, all adatoms and restatoms are of the same height, which is a simplification based on the image of empty states (Fig. 3, *a*). Contrary to this, the images of occupied states (Fig. 3, *d–f*) would suggest a lower height of adatoms and restatoms associated with the chain. It is important to stress that no conclusion can be reached on the basis of STM images alone, which are essentially a convolution of the topography and the electronic structure. As a further complication, the charge transfer from adatoms to restatoms in the region fo the linear chain is, obviously, of a lower magnitude than it is on the continuous c(2 × 8) or 2 × 2 areas. In general, establishing the exact atomic coordinates and electron wavefunctions within the models of Fig. 4 will require *ab initio* calculations of the optimized structural geometry and the electronic structure.

The formation of such linear 2 × 2 chain can be a model process of two-dimensional (2D) poly-crystalline growth. Namely, two translationally incoherent domains join their borders, as they grow in size during the final preparation stage of our sample. At 900 K, all adatoms may be considered mobile and are diffusing around on the top of the unreconstructed solid bulk. When the sample is slowly cooled down to 300 K, the adatoms lose their mobility and freeze in certain positions, by trying to saturate the dangling bonds of the substrate. Thus, a 2D crystal of adatoms is formed within the topmost layer of the c(2×8) reconstruction. Since adatoms' density is only one fourth of that on the bulk-like Ge(111) face, there are many equally suitable alternative positions, where such 2D crystal may start to nucleate. If it starts simultaneously on the opposite terrace boundaries, the nucleation sites may not be in accord with each other. Later on, when the crystallization proceeds into the middle of the terrace, there would be 2 × 2 chains from the left and from the right. When these two already crystallized regions meet each other, the area in between is smaller in width (marked as d in Fig. 4, *a*) than a single c(2 × 8) supercell. However, it is just right for the adatoms to be crystallized in the local 2 × 2 arrangement.

A related linear fault can be obtained on the ideally ordered Ge(111)-c(2 × 8) terrace by shifting an existing row of adatoms along the [1$\bar{1}$0] direction

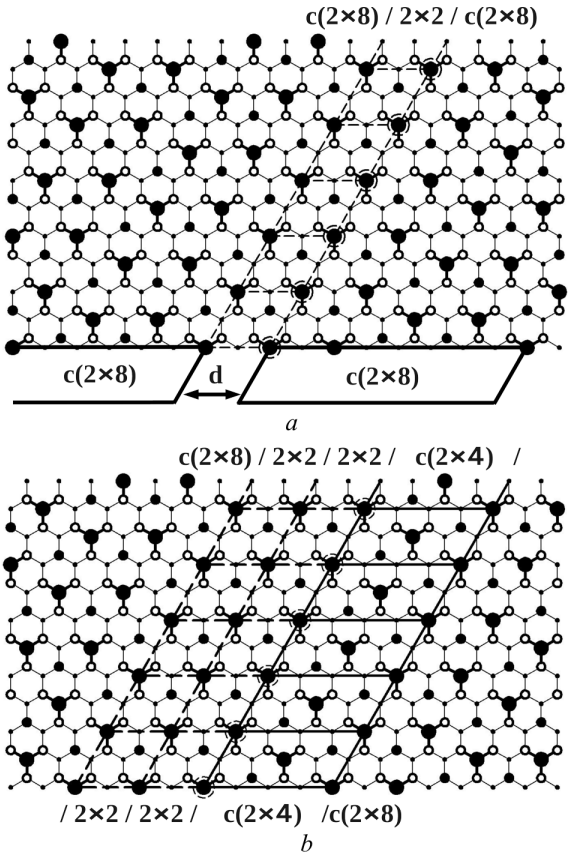

Fig. 4. Top views of the ball-and-stick atomic models of the Ge(111)-c(2 × 8) terrace with linear defects. The notation of Ge atoms is identical to that in Fig. 2. Adatoms belonging to the out-of-registry row are dash-encircled. Row of 2 × 2 supercells is designated by a dashed line, d is the shift between the c(2 × 8) registries on the left and on the right to the row; 2 × 2 and c(2 × 4) supercells outlined by dashed and solid lines, correspondingly (*a–b*)

by a single in-plane unit length of unreconstructed Ge(111). This is illustrated in Fig. 4, *b*, where the shifted adatoms are encircled by a dashed line. This shifting results in the splitting of every c(2×8) supercell, in which adatoms have been moved, into a pair of 2×2 cells (designated by a dashed line) and a single c(2 × 4) cell (designated by a solid line). In contrast to the case of Fig. 4, *a*, the c(2×8) domains to the left and to the right from this linear fault are naturally in registry with each other. The concerted shifting of the entire adatom row within the whole terrace is improbable, as it will require too much energy supplied to adatoms in a correlated manner. However, the adatoms can shift one by one, provided there is

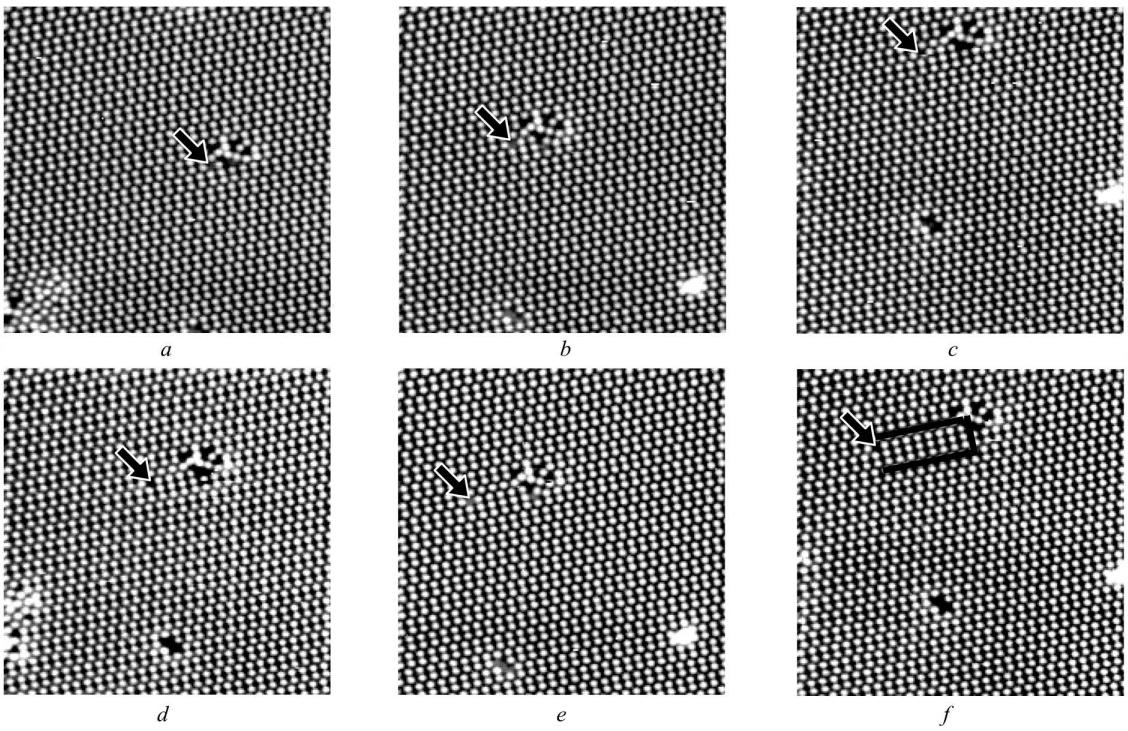

Fig. 5. STM images of the Ge(111)-c(2 × 8) terrace with adatoms shifted to different positions. All images are 25 nm × 25 nm in size and show the same area on the sample except for some shifts due to the thermal drift. The alphabetic ordering of images does not reflect the actual sequence, in which they were obtained. Sample bias voltages are: +1.5 V (*a*); +1.5 V (*b*); +1.7 V (*c*); +2.0 V (*d*); +1.8 V (*e*); +1.8 V (*f*). Tunneling current: 0.3 nA. In every panel, the location of the adatom vacancy involved in the row shifting is designated by a black arrow. In panel *f*, the black line designates the c(2 × 4) domain

an appropriate vacancy for the shift of at least one of them. This is illustrated in the consecutive panels of Fig. 5, where a c(2 × 8) terrace with a large adatom vacancy cluster is depicted.

Before discussing Fig. 5, it is worth to note that the STM images in its panels were not obtained in the alphabetic sequence *a*–*f*). Instead, they were hand-picked from a wider variety of STM images obtained in the course of time on the same surface area (except some thermal drifting) in order to reflect different stages of the process of diffusion of adatoms. This observation is fully in line with the previous report [18], where the adatom hoping on Ge(111)-c(2 × 8) was observed by STM at room temperature on the time scales of dozens of seconds. The activation energy was not derived in the study mentioned above, and the experiment was conducted in a manner similar to Fig. 5. Namely, the STM image was repeteadly obtained on the same surface area. Therefore, we cannot exclude that the activation energy is actually too high for the adatom diffusion at room temperature. However, it can still take place due to the interaction with the STM probe tip.

In Fig. 5, *a*, a vacancy, into which an adatom from the c(2 × 8) domain can diffuse, is marked by a black arrow in the central part of the image. In Fig. 5, *b*, this site is already filled by the neighboring adatom, and the vacancy itself is shifted to the left by two unreconstructed in-plane units. This process advances further also in panels *c* through *f*, while the black arrow marks the actual position of the vacancy in every image. In Fig. 5, *f*, the vacancy is eight "jumps" away from its initial position in Fig. 5, *a*, and the c(2 × 4) domain is outlined in black. Under the given experimental conditions, the adatoms can diffuse both to the right and to the left. Thus, the resulting (2 × 2)/(2 × 2)/c(2 × 4) linear fault can be of arbitrary length (naturally within the boundaries of the given terrace). This is an important difference to the 2 × 2 fault in Fig. 3, whose length being always

fixed by the points of its intersection with either terrace's or domain's boundaries.

5. Ge(111)-2 × 2 and Corner Holes

The deviations from the ideal Ge(111)-c(2 × 8) reconstruction discussed above were based on the linear (one dimensional, 1D) ordering of 2 × 2 supercells. New surface features can also arise on the boundaries of 2D 2 × 2 domains, which are generally rather small in their lateral size. This is vividly illustrated by STM images in Fig. 6, where a number of 2 × 2 domains is concentrated on a small area. Such areas could always have been found on the samples along with highly ordered c(2 × 8) areas. One of the possibilities for their mutual arrangement is the symmetric placement of six domains around a certain point. In Fig. 6, *a*, such arrangement is encircled by a black/white dashed line on the right side of the image. No adatom is visible in the central symmetry point, and it is encircled by six adatoms belonging to six participating 2 × 2 domains. This object looks very similar to the corner hole of the Si(111)-7 × 7 reconstruction. However, in the latter case, this is a regular periodic feature of the surface structure, while it is essentialy a defect in the present situation. Here, we deal with a rather peculiar case where the defect has a high symmetry (six-fold rotation), which is absent on the regular surface.

The specificity of the corner holes of the Si(111)-7 × 7 reconstruction is the absence of both adatoms and restatoms inside of them. Confirming this fact for such holes on Ge(111) requires the STM imaging both in empty and occupied states. Thus, we have obtained two STM images at sample bias voltages equal to –2.5 V (Fig. 6, *b*) and +2.5 V (Fig. 6, *c*) on the area containing the holes of various geometries. Comparing Fig. 6, *b* and *c*, one can notice that not every hole in the image of empty states looks like a hole in the image of occupied states. The holes, which are visible in both images, are marked by black arrows, including a symmetric one with 6 adatoms in the upper right corner of the captured area. The absolute value of bias voltage in Fig. 6, *b*–*c* (near the highest value, at which a stable imaging was possible for the given sample and probe tip) ensures that the wide enough range of electronic states around the Fermi level of the sample is involved in the image formation. Thus, there are no adatoms, restatoms, or any other atoms at similar heights within the holes marked by black arrows in Fig. 6, *b*–*c*.

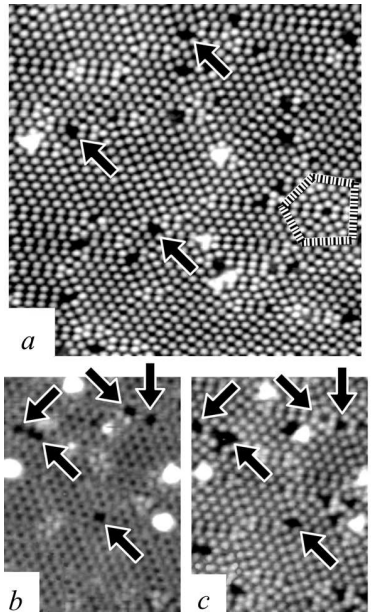

Fig. 6. STM images of the Ge(111) reconstructed surface with high numbers of domains and defects. 25 nm × 25 nm, sample bias voltage: +1.5 V, tunneling current: 0.3 nA (*a*); The black and white dashed line encompasses a symmetric corner hole, while black arrows point at non-symmetrical corner holes. 12.5 nm × 16.6 nm, –2.5 V, 0.3 nA (*b*); 12.5 nm × 16.6 nm, +2.5 V, 0.3 nA (*c*). Images *b*–*c* show the same surface area in occupied and empty states, correspondingly, black arrows point at various corner holes, which are present in both images

The experimental data presented above are the basis for the atomic model of an ideal symmetric corner hole (a direct counterpart of the Si(111)-7 × 7 corner hole) on the Ge(111) surface, which is depicted in Fig. 7. The model is derived from the 2×2 superstructure, which was shown in Fig. 2, *b*. In Fig. 7, there are a total of six 2×2 domains (identified by the adatoms numbering), their registry being derived from the positions of adatoms around the ideal corner hole designated by a black and white dashed line in Fig. 6, *a*. All domains are drawn to be of the same size, but, in reality, they can also be smaller or larger than depicted ones. In other words, the 2 × 2 superstructure can be translated closer or farther away from hole's center individually in each domain. In the minimal case, at least one adatom (nearest to the center encircled by the fine dashed line) should remain present from each domain. These six nearest adatoms form

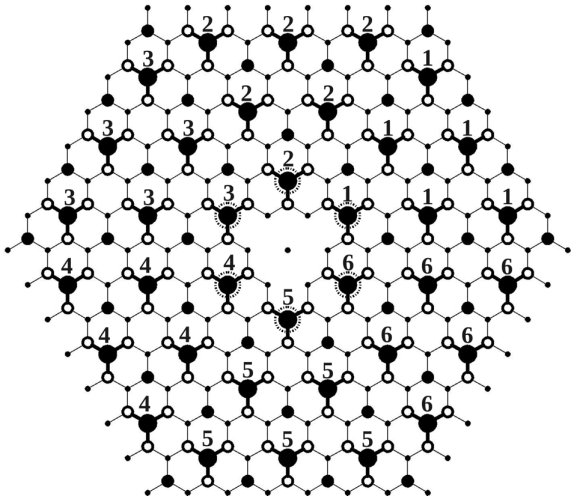

Fig. 7. Top view of the ball-and-stick model of the symmetric corner hole at the juncture of six 2×2 domains on Ge(111). The Ge atoms notation is identical to that in Fig. 2. Adatoms are numbered according to the 2×2 domain, which they belong to

a ring, which encircles the corner hole, and inside of which the restatoms are removed. Such removal impacts also those backbond atoms, which would have to be converted to restatoms, in the absence of adatoms). This removal leaves the only second layer atom (small black dot) at the center of the hole.

The structure suggested in Fig. 7 is substantially different from the established model of the corner hole on Si(111). The later has a threefold rotation symmetry due to the existence of a stacking fault, which is lower than the sixfold rotation in Fig. 7. Moreover, the suggested corner hole on Ge(111) is one layer shallower than in the case of Si(111): the central atom is only by three (instead of four on Si(111)-7×7) layers deeper than the adatoms. This difference is caused by the presence of the additional atomic layer with dimers between the faulted and unfaulted halves of the 7×7 unit cell. However, we do not claim that Fig. 7 presents a finally established model. Rather this is only the first tentative model based on a simple principle of removing both adatoms and restatoms inside the hole.

6. Adatom/Restatom Group Vacancies on Ge(111)

The STM data presented above indicate that the inventory of the reconstructed Ge(111) surface includes a variety of objects, which are similar in their nature to corner holes of Si(111)-7×7. The ideal corner hole, which looks identical to the Si(111)-7×7 corner hole in STM images is only one kind belonging to this type of objects. Other types are typically larger in the area encircled by more than 6 adatoms and of a less symmetric geometry arising at the junction points of not exclusively 2×2, but possibly also c(2×8) and/or c(2×4) domains. In Fig. 6, *a*, there are a number of such related features (some of them are designated by arrows), which produce a visual impression of holes in the uniform adatoms layer. In Fig. 7, the ideal corner hole of the highest symmetry is depicted, while atomic models of other holes can be constructed in a straightforward manner (they are not shown due to the extremely wide variety, which would hit the space limitation of a single paper). Actually, the best way of naming all of them is to use the term "adatom/restatom group vacancy". This means a limited area on the sample, where any atoms belonging to the layers of adatoms and restatoms have been removed and one or two deeper atomic layers are exposed to vacuum. The latter pricnciple is simultaneously a recipe for constructing the atomic model of every particular type of adatom/restatom group vacancy.

Similar to the Si(111)-7×7 corner holes, the atomic geometry of the adatom/restatom group vacancies prevents the deeper layer atoms inside of them from being imaged in STM due to the aspect ratio issues of the typical probe tips. In Si(111)-7×7 investigations, a special probe tip modified by the presence of a Bi atom on the apex was required to image a deep Si atom at the center of the corner hole and to study its chemical reactivity toward atomic hydrogen [19]. Thus, it will be extremely interesting to employ such modififed probe tips in future STM investigations of various adatom/restatom group vacancies on Ge(111). Despite some difficulty for the STM investigation, the specific atomic geometry discussed above gives rise to a new type of nanostructured Ge(111) surface with the lateral distance between the neighboring group vacancies to be in the range of several nm, as demonstrated in Fig. 6.

With c(2×8) being dominant on the Ge(111) surface, a question arises: where can 2×2 domains and adatom/restatom vacancy groups be found on the sample? A natural place to look for such objects are domain boundaries such as the steps between neighboring terraces or borders between differently

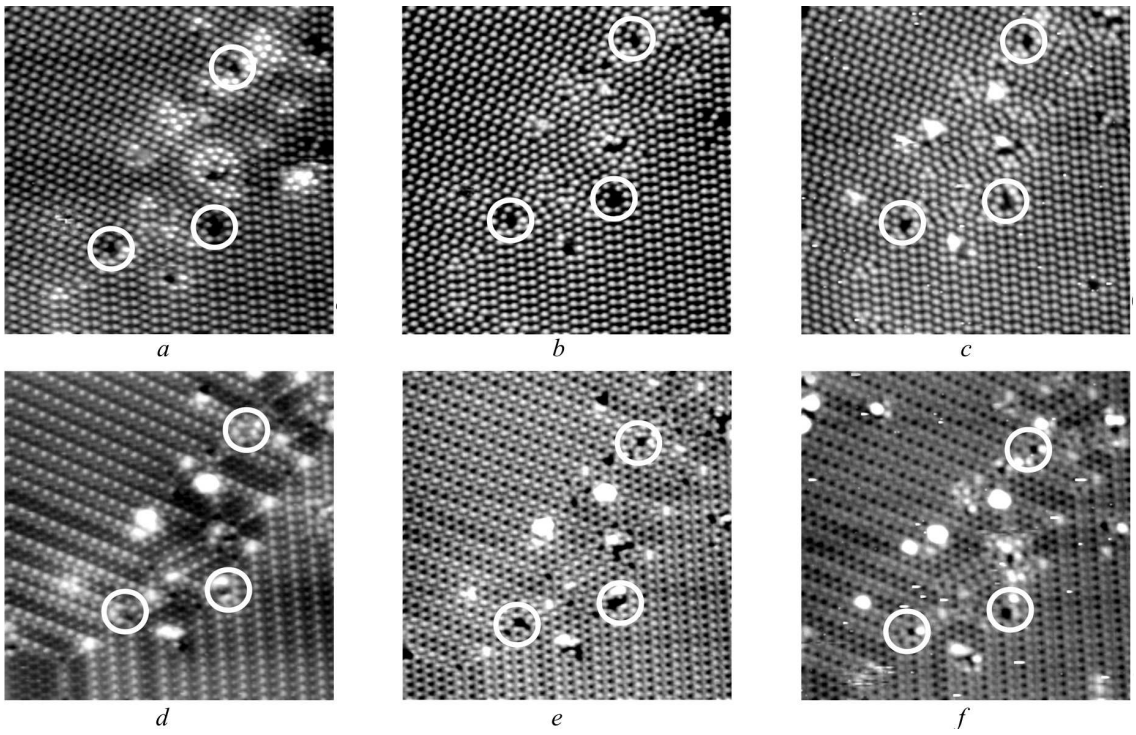

Fig. 8. STM images of the area on the Ge(111) sample, where two differently oriented c(2 × 8) domains meet each other. All images are 25 nm × 25 nm in size and show the same area on the sample except for some shifts due to the thermal drift. Sample bias voltages are: +1.0 V (*a*); +1.5 V (*b*); +2.5 V (*c*); −1.0 V (*d*); −1.5 V (*e*); −2.5 V (*f*). Tunneling current: 0.3 nA. In every panel, the location of the same three adatom/restatom vacancy groups is encircled in white

oriented c(2 × 8) domains within a single terrace, as Fig. 8 demonstrates. Here, the same surface area (with two c(2 × 8) domains "propagating" from upper left and lower right corners) is imaged in panels *a*–*f*) at different sample bias voltages. The two domains do not join each other along some well-defined line. Instead, a region of disorder appears along the diagonal of the imaged area, where adatom/restatom group vacancies are naturally present (three same group vacancies are encircled in every panel as a guide for an eye).

The differences in panels 8 *a*–*f* originate from the specific distribution of the local density of states on adatoms and restatoms. In empty states (panels *a*–*c*), there are only adatoms visible in the STM image, and they are all of equal brightness on the non-defect c(2 × 8) areas. In occupied states (panels *d*–*f*), both adatoms and restatoms contribute to the image formation. In the regular c(2 × 8) areas, they are roughly of the equal brightness for a high negative bias voltage (–2.5 V, panel *f*), while the image contrast is dominated by the asymmetry between restatoms within the c(2 × 8) unit cell at a low negative bias voltage (–1 V, panel *d*). In all panels of Fig. 8, the visible adatoms and restatoms within the defect area are of different brightnesses than on the regular c(2 × 8) areas. Furthermore, this difference is a function of the bias voltage. This means that a complicated redistribution of the local density of electronic states as a function of the energy takes place among the adatoms and restatoms in the partially disordered area in Fig. 8.

Different panels of Fig. 8 also demonstrate how the appearance of the adatom/restatom group vacancy in the STM image changes as the sample bias voltage is altered. While the shape of some group vacancy is the same for all three empty states images (Fig. 8, *a*–*c*) due to the invisibility of restatoms, it changes substantially in the images of occupied states (Fig. 8, *c*–*d*), when the restatoms become visible, each of them contributing differently to the tunneling current depending on the energy range of electronic states in-

volved in the process. Thus, the actual "hole" (as an object of a similar nature as the Si(111)-7 × 7 corner hole) can be rather small, actually of the smallest size selected from all images obtained at different voltages. However, this may not be applied to the images taken at low bias voltages, in particular, in Fig. 8, *d*, where the contrast due to the local density of electronic states between different groups of adatoms and restatoms is so strong, that it overshadows the topographic contrast, rendering the group vacancy almost invisible.

7. Discussion

It is worth mentioning that various types of adatom/restatom group vacancies (including ideal symmetric corner holes) were observed in our previous investigations on the Ge(111) surface with submonolayer bismuth coverage (see Fig. 4 in [20] and Figs. 5 and 6 in [21]). The presence of a Bi adsorbate (coverage between 0.05 and 0.25 monolayer) caused a substantial disorder of the uncovered substrate areas, becoming reach on small-size 2×2 domains, thus leading to the presence of group vacancies.

It seems reasonable that other impurities in moderate quantities (leaving enough the bare germanium substrate for observations) can also lead to the appearance of adatom/restatom group vacancies and ideal symmetrical corner holes. We speculate that other factors disturbing the surface structure (e.g., ion or electron bombardment) may also lead to such kind of nanostructuring of Ge(111). It is important, however, that any such influence is followed by the annealing, thus giving the surface a possibility to reconstruct back after a partial disordering, for instance, the 450 K annealing in the case of Bi adsorbates [20, 21]. The thermal dose should be just right to give the enough mobility to the Ge atoms in the surface layer to form a lot of small patches of the 2×2 reconstruction or/and small misoriented c(2×8) domains, but not enough to allow the return to the global surface free energy minimum with terrace size c(2×8) domains.

A special case is the strain-driven nanostructured Ge(111), which was practically realized by growing a Ge film on the top of the Si(111)-7 × 7 substrate [22]. The strained germanium film develops a surface with 5×5 and 7×7 dimer – adatom – stacking fault reconstruction (thus, with a regular array of ideally symmetric corner holes), as well as a rich variety of small 2×2, c(2×4) and c(2×8) domains. Therefore, one might also expect to observe such structures on a single crystal Ge(111), if the experimental difficulties of preparing the sample under an externally introduced mechanical stress in ultra-high vacuum are overcome.

The future experiments may exploit the Ge(111)-c(2×8) reconstructed surface with linear 2×2 chains and dimer/adatom group vacancies as a chemically homogeneous template for creating the one- or two-dimensional arrays of adsorbed species. A distinct electronic structure of a 2×2 chain, which manifests itself in Fig. 3, can act as a selective adsorption site for certain atomic or molecular species, thus arranging the adsorbates according to the linear geometry of the chain. In its turn, the dimer/adatom group vacancies, if produced with significant surface density, can host molecules or atomic clusters of an appropriate size, by creating a surface array of such molecular clusters.

Apart from group vacancies and linear chains, other defects found on the STM images presented above include the domain boundaries and the joint points of various 2×2, c(2×4) and c(2×8) domains. These defects can also possess some specific adsorption properties and can be targeted in future studies of atomic and molecular adsorptions. Due to the typical sizes of such defects in the nm range, the adsorbates with preferrential adsorption on the top of them will form various nano-sized aggregates, which can enhance the nanostructuring of Ge(111).

Another direction of future researches may focus on the adatom vacancy diffusion and the $(2 \times 2)/(2 \times 2)/\mathrm{c}(2 \times 4)$ chain of fluctuating length. Here, a technique similar to the atom-tracking STM developed by Swartzentruber [21] may be helpful. However, this will require a modification of the tracking technique, which was originally designed to follow a single atom adsorbed on the top of an atomically flat terrace. There seems no principal obstacle to convert it in a way where a vacancy (a pit instead of a hill amidst a plane) will be targeted.

8. Conclusions

We have presented the STM observations (including the voltage-dependent imaging) of both 1- and 2-dimensional nanostructuring of the atomically clean single crystal Ge(111)-c(2×8) substrate prepared by

the high-temperature (900 K) annealing under UHV conditions. The most spectacular features arise due to locally stabilized patches of 2×2 reconstruction and include 1D "antiwires" of 2×2 unit cells and corner holes at the joining points of six 2×2 domains. The atomic models of these objects are empirically derived from the STM images obtained at various bias voltages and will have to be confirmed by *ab initio* structural calculations in future studies. In addition, the ideal symmetric corner holes are further generalized to a wider class of adatom/restatom group vacancies, which are characterized with STM in a comprehensive manner.

All STM data processing was performed using the Gwyddion software package, which is available as "open source" and can be downloaded from the gwyddion.net website. We are thankful to Dr. I. Lyubinetsky for generously providing the Ge(111) wafers.

1. C.B. Duke, Chem. Rev. **96**, 1237 (1996).
2. G. Binnig, H. Rohrer, Ch. Gerber *et al.*, Phys. Rev. Lett. **50**, 120 (1983).
3. K. Takayanagi and Y. Tanishiro, Phys. Rev. B **34**, 1034 (1986).
4. R.S. Becker, B.S. Swartzentruber, J.S. Vickers *et al.*, Phys. Rev. B **39**, 1633 (1989).
5. E.S. Hirschorn, D.S. Lin, F.M. Leibsle *et al.*, Phys. Rev. B **44**, 1403 (1991).
6. R.M. Feenstra, G. Meyer, F. Moresco *et al.*, Phys. Rev. B **64**, 081306R (2001).
7. W.S. Verwoerd, V. Nolting, P. Badziag, Surf. Sci. **241**, 135 (1991).
8. G. Lee, H. Mai, I. Chizhov *et al.*, J. of Vac. Sci. and Techn. A **16**, 1006 (1998).
9. G. Lee, H. Mai, I. Chizhov *et al.*, Surf. Sci. **463** 55 (2000).
10. I.V. Lyubinetsky, P.V. Melnik, N.G. Nakhodkin *et al.*, Vacuum **46**, 219 (1995).
11. I. Razado-Colambo, J. He, H. Zhang *et al.*, Phys. Rev. B **79**, 205410 (2009).
12. P. Molinas-Mata, J. Zegenhagen, Solid State Comm. **84**, 393 (1992).
13. D.J. Chadi ,and C. Chiang, Phys. Rev. B **23**, 1843 (1981).
14. D. Drakova and G. Doyen, Progr. Surf. Sci. **46** 251 (1994).
15. T.M. Jung, R.J. Phaneuf, and E.D. Williams, Surf. Sci. **254** 235 (1991).
16. N. Takeuchi, A. Selloni, and E. Tosatti, Phys. Rev. Lett. **69** 648 (1992).
17. R. Feidenhans'l, J.S. Pedersen, J. Bohr *et al.*, Phys. Rev. B **38**, 9715 (1988).
18. A.J. Mayne, F. Rose, C. Bolis *et al.*, Surf. Sci. **486**, 226 (2001).
19. S.Yu. Bulavenko, P.V. Melnik, M.G. Nakhodkin *et al.*, Surf. Sci. **600**, 1185 (2006).
20. A. Goriachko, P.V. Melnik, A. Shchyrba *et al.*, Surf. Sci. **605**, 1771 (2011).
21. A. Goriachko, A. Shchyrba, P.V. Melnik *et al.*, Ukr. J. Phys. **59** 805 (2014).
22. U. Köhler, O. Jusko, G. Pietsch *et al.*, Surf. Sci. **248** 321 (1991).
23. B.S. Swartzentruber, Phys. Rev. Lett. **76** 459 (1996).

Received 25.01.15

А. Горячко, П.В. Мельник, М.Г. Находкін

ДОСЛІДЖЕННЯ НОВИХ ОСОБЛИВОСТЕЙ ПОВЕРХНІ Ge(111) ЗІ СПІВІСНУЮЧИМИ РЕКОНСТРУКЦІЯМИ c(2 × 8) ТА 2 × 2 МЕТОДОМ СКАНУВАЛЬНОЇ ТУНЕЛЬНОЇ МІКРОСКОПІЇ

Р е з ю м е

Реконструйована поверхня Ge(111) може легко переходити з основного стану із суперкоміркою c(2 × 8) у збурений стан 2 × 2 внаслідок близькості їхніх значень поверхневої вільної енергії. Ці дві реконструкції поверхні германію є достатньо вичерпно вивченими в попередніх роботах, проте нові структурні особливості можуть бути знайдені на границях між доменами c(2 × 8) та 2 × 2 із різноманітними орієнтаціями та латеральними зсувами. Наведено результати досліджень методом сканувальної тунельної мікроскопії та запропоновано атомні моделі лінійних ланцюжків комірок 2 × 2 або c(2 × 4), а також адатомно-рестатомних групових вакансій, включаючи кутові ями із аналогічною геометрією як у випадку поверхні Si(111)-7 × 7.

А. Горячко, П.В. Мельник, М.Г. Находкин

ИССЛЕДОВАНИЕ НОВЫХ ОСОБЕННОСТЕЙ ПОВЕРХНОСТИ Ge(111), СОДЕРЖАЩЕЙ СОСУЩЕСТВУЮЩИЕ РЕКОНСТРУКЦИИ c(2 × 8) И 2 × 2, МЕТОДОМ СКАНИРУЮЩЕЙ ТУННЕЛЬНОЙ МИКРОСКОПИИ

Р е з ю м е

Реконструированная поверхность Ge(111) может легко переходить из основного состояния с суперрешеткой c(2 × 8) в возмущенное состояние 2 × 2 вследствие близости их значений поверхностной свободной энергии. Эти две реконструкции поверхности германия были исчерпывающе изучены в предыдущих работах, однако новые особенности могут быть найдены на границах между доменами c(2 × 8) и 2×2 с разнообразными ориентациями и латеральными сдвигами. Приводятся результаты исследований методом сканирующей туннельной микроскопии и предложены атомные модели линейных цепочек ячеек 2 × 2 или c(2 × 4), а также адатомно-рестатомных вакансий, включая угловые ямы аналогичной геометрии как и в случае поверхности Si(111)-7 × 7.